

Thermal conductivity estimates in the Niger Delta using lithologic data and geophysical well logs

Author(s): Idara Akpabio and Joe Ejedawe

Source: *Current Science*, Vol. 98, No. 3 (10 February 2010), pp. 411-417

Published by: Current Science Association

Stable URL: <https://www.jstor.org/stable/24111591>

Accessed: 01-06-2021 11:17 UTC

JSTOR is a not-for-profit service that helps scholars, researchers, and students discover, use, and build upon a wide range of content in a trusted digital archive. We use information technology and tools to increase productivity and facilitate new forms of scholarship. For more information about JSTOR, please contact support@jstor.org.

Your use of the JSTOR archive indicates your acceptance of the Terms & Conditions of Use, available at <https://about.jstor.org/terms>



JSTOR

Current Science Association is collaborating with JSTOR to digitize, preserve and extend access to *Current Science*

11. Ray, J. S. and Ramesh, R., Rayleigh fractionation of stable isotopes from a multicomponent source. *Geochim. Cosmochim. Acta*, 2000, **64**, 299–306.
12. Albarede, F., *Introduction to Geochemical Modeling*, Cambridge University Press, UK, 1995, pp. 47–50.
13. Richards, F. A., Anoxic basins and fjords. In *Chemical Oceanography* (eds Riley, J. P. and Skirrow, G.), Academic Press, 1965, vol. 1, pp. 611–645.
14. Payne, W. J., Reduction of nitrogenous oxide by micro-organisms. *Bacteriol. Rev.*, 1973, **37**, 409–452.
15. Cline, J. D. and Richards, F. A., Oxygen deficient conditions and nitrate reduction in the eastern tropical North Pacific Ocean. *Limnol. Oceanogr.*, 1972, **17**, 885–900.
16. Naqvi, S. W. A., Some aspects of the oxygen deficient conditions and denitrification in the Arabian Sea. *J. Mar. Res.*, 1987, **45**, 1049–1072.
17. Brandes, J. A., Devol, A. H., Yoshinari, T., Jayakumar, D. A. and Naqvi, S. W. A., Isotopic composition of nitrate in the central Arabian Sea and eastern tropical North Pacific: A tracer for mixing and nitrogen cycles. *Limnol. Oceanogr.*, 1998, **43**, 1680–1689.
18. Delwiche, C. C. and Steyn, P. L., Nitrogen isotope fractionation in soils and microbial reactions. *Environ. Sci. Technol.*, 1970, **4**, 929–935.
19. Mariotti, A., Germon, J. C., Hubert, P., Kaiser, P., Letolle, R., Tardieux, A. and Tardieux, P., Experimental determination of nitrogen kinetic isotope fractionation: some principles; illustration for the denitrification and nitrification processes. *Plant Soil*, 1981, **62**, 413–430.
20. Barford, C. C., Montoya, J. P., Altabet, M. A. and Mitchell, R., Steady-state nitrogen isotope effects of N_2 and N_2O production in *Paracoccus denitrificans*. *Appl. Environ. Microbiol.*, 1999, **65**, 989–994.
21. Blair, N., Leu, A., Munos, E., Olsen, J., Kwong, E. and Des Marais, D., Carbon isotopic fractionation in heterotrophic microbial metabolism. *Appl. Environ. Biol.*, 1985, **50**, 996–1001.
22. Cleixner, C., Danier, H. J., Werner, R. A. and Schmidt, H. L., Correlations between the ^{13}C content of primary and secondary plant products in different cell compartments and that in decomposing basidiomycetes. *Plant Physiol.*, 1993, **102**, 1287–1290.
23. Accoe, F., Boeckx, P., Cleemput, O. V., Hofman, G., Zhang, Y., Li, R. H. and Guanxiong, C., Evolution of the $\delta^{13}C$ signature related to total carbon contents and carbon decomposition rate constants in a soil profile under grassland. *Rapid Commun. Mass Spectr.*, 2002, **16**, 2184–2189.

ACKNOWLEDGEMENT. We are grateful to the anonymous reviewers for their critical comments.

Received 10 July 2009; revised accepted 7 January 2010

Thermal conductivity estimates in the Niger Delta using lithologic data and geophysical well logs

Idara Akpabio^{1,*} and Joe Ejedawe

Exploration Department, Shell Petroleum Development Company, Port Harcourt, Nigeria

¹Permanent address: Department of Physics, University of Uyo, Nigeria

Thermal rock properties and heat flow were determined from 260 wells in the Niger Delta. The thermal conductivity data provides inputs for the determination of heat flow and for thermal evaluation of the Niger Delta basin. A map has been constructed using lithologic data and geophysical well logs to give an overview of its distribution. The thermal conductivity for sand and shale, the predominant lithology in the Niger Delta, shows wide variations from one well to another. In the Benin Formation, thermal conductivity has an average value of 8 W/mK. The lowest values are found offshore westward, while highest values occur northward. The conductivity values, however, decrease towards the marine paralic section, with an average value of 5 W/mK, the region of highest interest. The thermal conductivity values have been used in calculating heat flow. A significant regional trend of relatively low (20–30 mW/m²) heat flow at the central part of the delta, increases both seaward and northward (40–55 mW/m²). The lowest values of heat flow as low as 20 mW/m² are recorded in the central part of the delta while the highest values exceeding 50 mW/m² are recorded in the northern part of the delta. Knowledge of thermal properties has direct relevance for hydrocarbon exploration. It has been established that the bulk of hydrocarbon accumulation in the Niger Delta is of thermal origin, hence the importance of this findings.

Keywords: Heat flow, temperature, thermal conductivity, sand percentage.

THE thermal conductivity of rocks is one of the major factors that affect temperature in sedimentary basins and therefore, should be addressed in basin analysis; its effect on the temperature distribution is significant, up to the order of 50–80%¹. As a result of thermal conductivity, thermal structure of a basin may change laterally and vertically even if the heat flow into the basin is regionally the same².

The variability of heat flow in most basins must arise from some combination of at least the following four principal influences: heat redistribution by migration of formation fluids (hydrodynamic effect); variations in conductivity and heat generation in the sedimentary

*For correspondence. (e-mail: idara_akpabio@yahoo.com)

succession; variations in the heat generation of crystalline basement, and variations in mantle heat flow³.

Here, we present thermal conductivity profiles from lithologic information and continuous temperature data across the Niger Delta basin covering the area bounded between lat. 5°38'–6°00'N and long. 5°38'–6°43'E (Figure 1).

The geologic setting of the Niger Delta basin is well documented in the literature⁴. In summary, three main lithostratigraphic units have been recognized and were laid down under Marine, Transitional and Continental environments corresponding to Akata, Agbada and Benin formations.

Akata Formation is the basal sedimentary unit, composed mainly of marine shales. The shales are undercompacted and may contain abnormally high-pressured siltstone or fine-grained sandstone. It is believed to be the main source rock for the Delta and the basic unit of the Cenozoic complex. It ranges in thickness approximately from 600 to 6000 m.

Agbada Formation consists of alternations of sands, sandstones and siltstones. Due to differential subsidence variations in the sediment, Agbada sandstone is poorly sorted with various grain sizes ranging from fine to coarse whereas its sands contribute the main hydrocarbon reservoir of the Delta. The consolidated sands have a calcareous matrix, shale fragments and glauconite occur while lignite streaks and limonite are common. The thickness ranges approximately from 2880 to 4200 m while the age ranges from mid-Miocene to late-Miocene.

Benin Formation is the uppermost limit of the Delta as thick as 3000 m and extends to about 9730 m out of the Bonny beach. The sands and sandstones range from coarse to fine and are poorly sorted showing a little lateral continuity⁴.

1. The sand/shale percentage data were interpreted from three types of lithologic logs: resistivity, gamma ray and spontaneous potential for 260 wells widely spread

across the Niger delta (Figure 2). (i) Resistivity logs are electric logs used to indicate permeable zones (such as sand) from impermeable zones (such as shale). (ii) Gamma ray log is a measurement of intensity of natural gamma radiations spontaneously emitted by some radioactive elements like shales and clay⁵. Shale-free sandstones have low concentration of radioactive material. (iii) A spontaneous log primarily identifies impermeable zones (shale) from permeable zones (sand).

2. Continuous temperature logs were also interpreted for the same number of wells. The temperature logs were more reliable because they were recorded several months after wells have been drilled, so formation had stabilized. They were more reliable than Bottom Hole Temperatures.

3. Interval transit times were also collected for the same wells; it assisted in explaining certain anomalies. Interval transit time is the reciprocal of sonic velocity. It is determined from sonic well logs and used to estimate porosity of formations.

The Geometric Mean Model⁶ was used in this study. For rock porosity ϕ , the bulk conductivity of the porous rock K_r may be calculated as the geometric mean from phase conductivities, according to their fractional volume:

$$K_r = K_w \phi, K_s^{(1-\phi)}$$

$$\phi = 0.25 \exp(-z/3.0),$$

where ϕ is the porosity, K_w the conductivity of the fluid, Z the depth in km, K_s the matrix conductivity, $K_w = 0.56 + 0.003T^{0.827}$, for $0 \leq T \leq 63^\circ\text{C}$, $K_w = 0.481 + 0.942 \ln T$, for $T > 63^\circ\text{C}$.

Water has a given temperature dependence, although the effect is very small relative to temperature effects on the matrix conductivity. Water has a conductivity of 0.56 W/mK at 0°C that increases to 0.68 W/mK at 100°C. Water temperature conductivity are approximated by the following functions⁷,

$$K_w = 0.56 + 0.003T^{0.827}, \text{ for } 0 \leq T \leq 50^\circ\text{C},$$

$$K_w = 0.442 + 0.519 \ln T, \text{ for } T > 50^\circ\text{C},$$

K_s = Matrix conductivity given as

$$K_{sT} = K_{s20} (293/(273 + T)),$$

where K_{sT} is the matrix conductivity at temperature T (°C).

The geometric mean model formed the basis of an algorithm called LITHTEMP⁸. Figure 3 shows the flow line of the algorithm. In Figure 3: f_s, f_{sh} = fractional percentage of sand and shale (interpreted from gamma ray and resistivity logs for the 83 wells). f'_s and f'_{sh} are

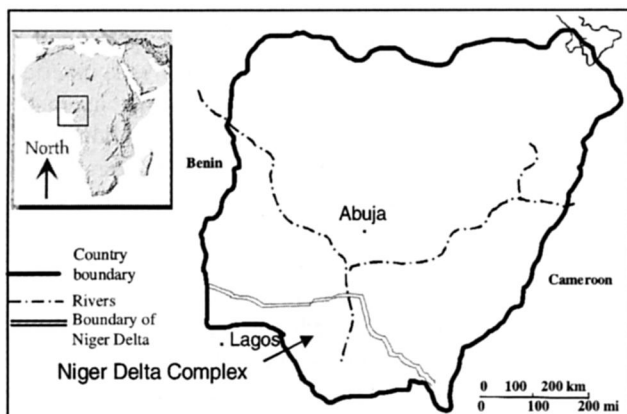


Figure 1. Location map of the Niger Delta region.

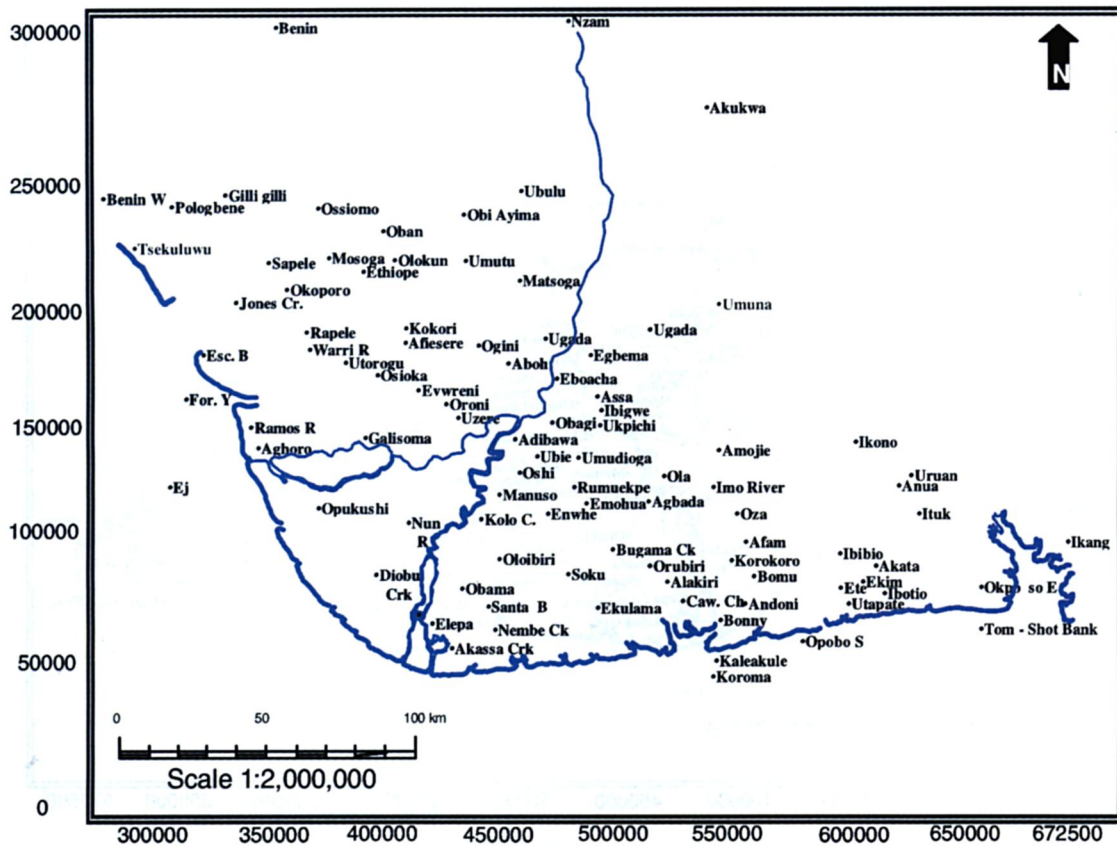


Figure 2. Location map of the Niger Delta showing wells used in the study.

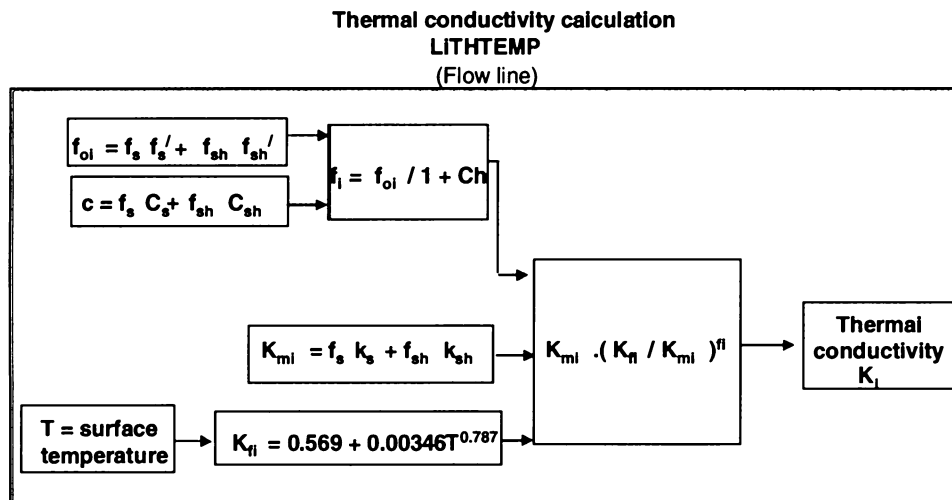


Figure 3. Algorithm for thermal conductivity calculation.

surface porosity of sand and shale (0.4 and 0.7; ref. 8) respectively. f_{oi} is the surface porosity of the interval; f_i the porosity of the i th interval; h the depth of selected interval (100 ft). C_s and C_{sh} are compaction coefficient of sand and shale (0.0012 and 0.0024; ref. 8) respectively; C_i the compaction coefficient of interval; K_{mi} the matrix

thermal conductivity of the i th interval; K_s and K_{sh} are assumed value of reference matrix thermal conductivity for sand and shale (6.1 W/mK and 2.1 W/mK) respectively¹; K_{fi} the thermal conductivity of water at temperature of interval; K_i the effective thermal conductivity; T the surface temperature.

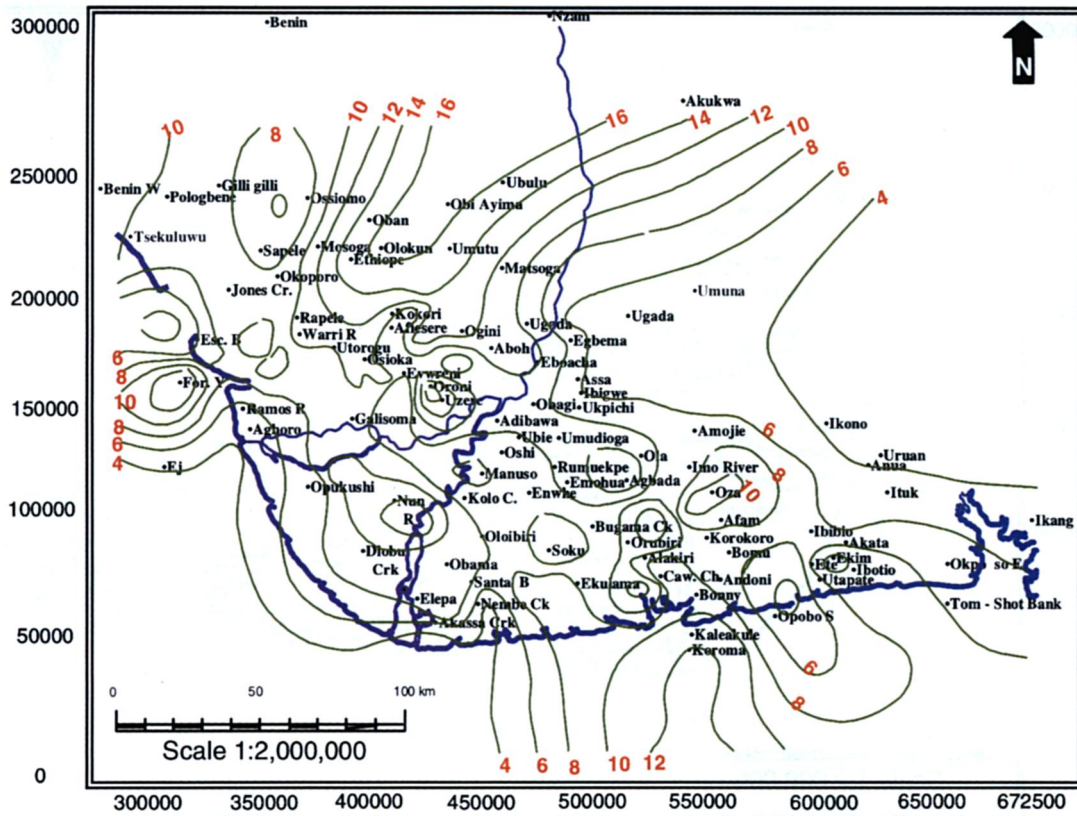


Figure 4. Thermal conductivity profile in the study area (shallow section).

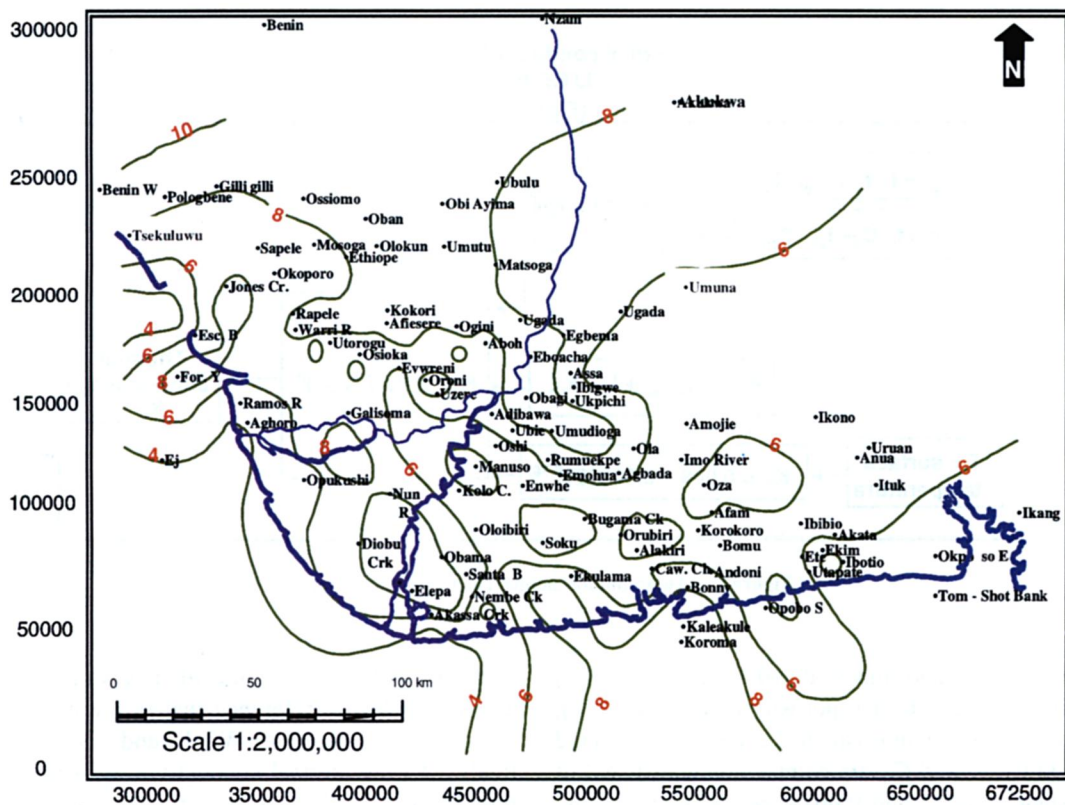


Figure 5. Thermal conductivity profile in the Machine paralic (deeper section).

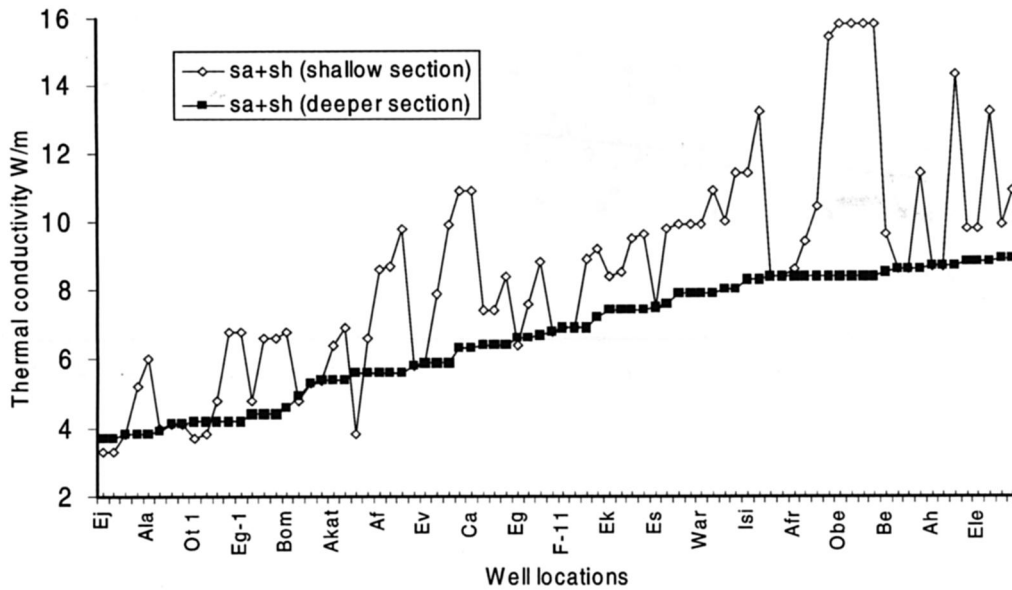


Figure 6. Thermal conductivity as a function of depth.

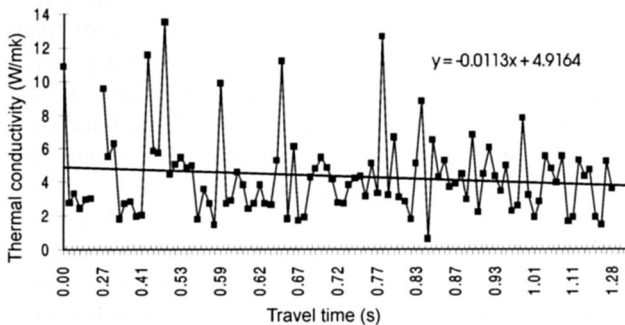


Figure 7. Thermal conductivity (sand and shale) versus travel time.

Heat flow q_i in any interval is then computed from the effective thermal conductivity K_i of the interval using the simple relation:

$$q_i = g_i K_i,$$

where g_i is the geothermal gradient of the interval. The geothermal gradient values used in this study were obtained from Akpabio *et al.*⁹.

The porosity calculation in the formula is based on the assumption that incremental change in porosity is proportional to change in load and to the ratio of void space to skeleton volume.

It is important to note that due to differences in the heat flow between formations, data were collected and results are presented in two different depth sections: in the Benin Formation (top to base continental sequence) and from base continental (mostly from 2000 ft) to continuous shale.

The thermal conductivity for sand and shale, the predominant lithology in the Niger Delta, shows wide varia-

tions from one well to another. Figures 4 and 5 show these areal variations. In the Benin Formation, conductivity ranges from 5 ± 2 to 10 ± 4 W/mK with an average of 8 W/mK. The lowest values were found offshore westward, whereas the highest values occur northward. The conductivity values, however, decrease when one approaches the marine paralic section with an average value of 5 W/mK.

However, some wells exist where thermal conductivity of the shallow section is lower than in the deeper section or conversely the heat flow is greater in the shallow portions of the well. Examples may be cited from the offshore depobelt. Depobelts are basinal areas emphasizing the genetic relationship between a structure and stratigraphy. There is a corresponding decrease in the travel time of sound waves in such areas; this may be associated with loss or absence of porosity within the interval. The regional distribution of thermal conductivity shows a variation with well location (Figure 6). These variations are inferred to relate to variations in the lithologies encountered.

In Brunei continental margin, the active fluid loss from depth (porosity) is the prime factor influencing the distribution of heat flow and thermogenic surface hydrocarbons¹⁰. Thermal conductivity varies with depth due to variable lithology and water content³.

The results from our analysis further confirm that all pore fillers are very poor conductors, i.e. thermal conductivity decreases with increasing porosity.

It has been shown that porosity decreases with increase in velocity and conversely the interval transit time¹¹. From our results, the thermal conductivity exhibits no direct or distinct relationship with sound travel time. However, in Figure 7, based on the trend line equation, $y = 0.0113x + 4.9164$, travel time decreases correspond-

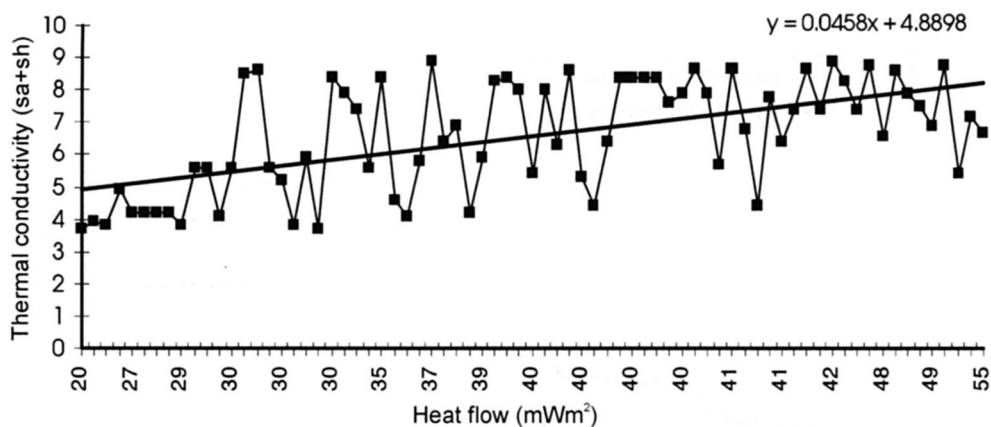


Figure 8. Heat flow versus thermal conductivity (sa + sh) Marine Formation.

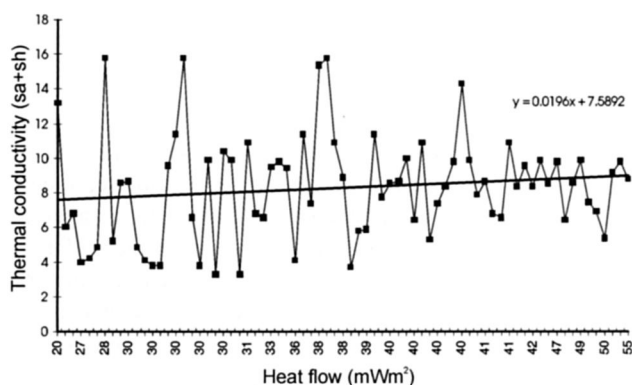


Figure 9. Heat flow versus thermal conductivity (sa + sh) Benin Formation.

ingly with low thermal conductivity. Since velocity increases with more compaction, transit time conversely reduces.

In Figure 6, thermal conductivity in the shallow Benin Formation is higher (average of 8 W/mK) than in the deeper marine paralic section (average of 6 W/mK). This presentation suggests that the Benin sands are more conducting than the marine shales.

Figure 6 also confirms that the high conductivity of the well conducting rocks decreases with increasing temperature, since temperature increases with depth. This is clearly shown as data for the deeper section has low thermal conductivity. This implies that large conductivity contrasts between various rock types are a shallow phenomenon (as can be seen on the scattered graph). It has been documented that the shallow Moho depth area of the Republic of Korea tends to have higher heat flow than the area of thick crust¹², a further confirmation of Figure 6.

It is worthy to point out the great thermal conductivity anisotropy exhibited at the shallow depth. Thermal conductivity anisotropy is a function of rock mineralogy and fabric¹³, particularly the bedding planes of the rock. However, thermal conductivity anisotropy is especially

pronounced in shales and clay-rich rocks¹⁴. On the contrary, Figure 6 shows less anisotropy in the shale-prone area, i.e. deep section of the formation.

Thermal conductivity and heat flow have a close relationship. Figure 8 shows that where there is a relatively low conductivity, heat flow is also low, similarly, where there is relatively high conductivity, heat flow is also high in the marine shale formation. The Benin Formation, however, shows a less definitive relationship compared to the marine section.

Heat flow varies from 20 to 55 mW/m², with an average of 36 mW/m² but is mostly in the 30–45 mW/m² range. Very large variation of heat flow suggests a large imprint of the highly variable heat generation in the upper crust. It is worthy of note that a hydrodynamic (fluid flow) effect superimposed on a generally high heat flow background (hot crust and upper mantle) is a possible influence³. The lowest heat flow is observed in the southern and offshore regions of the study area; Ej and Ea, Nun River and Alakiri. The highest heat flow is observed in the north; Tsekelewu, Benin West and Pologbene, with values exceeding 50 mW/m².

These boundaries suggest a difference between crustal blocks, characterized by contrasting heat generation. However, correlation with the regional magnetic anomaly signature, corresponding to units of the cratonic basement, is not obvious at this scale¹⁵.

Heat flow variations correspond to variations in geothermal gradient. Regional gradients are lowest (0.82°C/100 m) at the central part of the Delta and increases both seaward and northward up to 2.62°C/100 m and 2.95°C/100 m respectively in the continental sands of the Benin Formation. In the marine paralic deposition, geothermal gradients range from 1.83°C/100 m to 3.0°C/100 m at the central portions. The highest values of 3.5°C/100 m to 4.6°C/100 m are seen northwards while intermediate values of 2.0°C/100 m to 2.5°C/100 m are recorded seaward. The thermal gradients are clearly influenced by the lithology or rate of sedimentation in the area. Regions of

low thermal gradients correspond with areas of high sand percentage, primarily because sands are better conductors than shale and therefore show as low thermal gradients⁹.

1. Thermal conductivity varies with depth due to variable lithology and water content, from 8 W/mk in the Benin Formation to 5 W/mk in the marine shale formation.
2. Thermal conductivity calculations were based on assumed matrix conductivity of sand 6.1 W/mk and shale 2.1 W/mk, predominant lithologies in the Niger Delta.
3. Heat flow derived from thermal conductivity estimates at the central part of the Delta is 20–30 mW/m², it increases both seaward and northward to (40–55 mW/m²).
4. Thermal conductivity decreases with increase in temperature.
5. Thermal conductivity contrast between rock types is a shallow phenomenon.
6. Heat flow corresponds to variations in geothermal gradient.

1. Akpabio, I. O. and Ejedawe, J. E., Temperature variations in the Niger delta subsurface from continuous temperature logs. *Global J. Pure Appl. Sci.*, 2001, **7**, 137–142.
2. Norden, B. and Forster, A., Thermal conductivity and radiogenic heat production of sedimentary and magmatic rocks in the North-east German Basin. *AAPG Bull.*, 2006, **90**, 939–962.
3. Majorowicz, J., Jessop, A., Lane, A. M. and Larry, S., Regional heat flow pattern and lithospheric geotherms in Northeastern British Columbia and adjacent northwest territories, Canada. *Bull. Can. Pet. Geol.*, 2005, **53**, 51–66.
4. Reijers, T. J. A., Petters, S. W. and Nwajide, C. S., The Niger Delta basin. In *African Basins, Sedimentary Basins of the World* (ed. Selley, R. C.), 1997, vol. 3, pp. 145–172.
5. Schlumberger, *Log Interpretations, Principles and Applications*, Schlumberger Education Services, Houston, Texas, 1989.
6. Chapman, D. S., Keho, T. H., Bauer, M. S. and Picard, M. D., Heat flow in the Uinta Basin determined from BHT data. *Geophysics*, 1984, **49**, 453–466.
7. Briguad, F., Chapman, D. S. and Douaran, S. L., Estimating thermal conductivity in sedimentary basins using lithologic data and geophysical well logs. *AAPG*, 1990, **74**, 1459–1477.
8. Ejedawe, J., LITHTEMP, pers comm. Exploration Department, Shell Petroleum Development Company, Warri, 1997.
9. Akpabio, I. O., Ejedawe, Ebeniro, J. O. and Uko, E. D., Geothermal gradients in the Niger delta basin from Continuous temperature logs. *Global J. Pure Appl. Sci.*, 2003, **9**, 265–272.
10. Zielinski, G. W., BJORoy, M., Zielinski, R. L. B. and Ferriday, I. L., Heat flow and surface hydrocarbons on the Brunei continental margin. *AAPG Bull.*, 2007, **91**, 1053–1080.
11. Berge, P. A., Bomer, B. P. and Berryman, J. G., Ultrasonic velocity porosity relationship for sandstones analog made from fused glass beads. *Geophysics*, 1995, **60**, 108–119.
12. Kim Hyoung, C. and Lee Youngmin, Heat flow in the Republic of Korea. *J. Geophys. Res.*, 2007, **112**, B05413.
13. Pribnow, D. and Umsonst, T., Estimation of thermal conductivity from the mineral composition: influence of fabric and anisotropy. *Geophys. Res. Lett.*, 1993, **20**, 2199–2202.
14. Davies, M. G., Chapman, D. S., Wagoner, T. M. Van and Armstrong, P. A., Thermal conductivity anisotropy of metasedimentary and igneous rocks. *J. Geophys. Res.*, 2007, **112**, B05216.

15. Pilkington, M., Miles, W. F., Ross, G. M. and Roest, W. R., Potential-field signatures of buried Precambrian basement in the Western Canada Sedimentary Basin. *Can. J. Earth Sci.*, 2000, **37**, 1453–1471.

ACKNOWLEDGEMENT. We thank the SPDC, Nigeria for allowing the use of their facilities and access to the data on which this study was based.

Received 8 July 2008; revised accepted 30 September 2009

Comparative assessment of micro-watershed silt load with morphological parameters to evaluate soil conservation strategies

Praveen G. Saptarshi* and
Rao Kumar Raghavendra

Department of Environmental Sciences, University of Pune,
Pune 411 007, India

The comparative assessment of morphologic runoff and annual silt load from micro-watersheds can help in establishing relationships between these parameters with objectives of controlling runoff, conservation of soil, reduction of reservoir silt load and enhanced groundwater resources in the micro-watersheds. The automated watershed delineation technique using the filled digital elevation model is observed to be reliable for area having converging slopes. The estimation of watershed based annual silt load using universal soil loss equation along with runoff estimation utilizing the soil conservation services model using remote sensing data is possible on such automatically delineated micro-watershed groups. This can be validated through ground measurements. The output in raster geographic information system (GIS) is highly beneficial in making an inventory of soil loss, runoff and morphologic parameters with an objective of establishing relationship between these parameters for planning conservation measures. The GIS output products like soil-erosion potential map, run-off potential map, etc. obtained by using raster interpolation techniques are of value addition for developing and harnessing natural resources enabling sustainable development.

Keywords: Automated watershed delineation, comparative assessment, morphologic parameters, peak runoff, rainfall intensity, soil erosion, surface interpolation.

LAND evaluation is necessary to assess the potential constraints of a given piece of land¹. Watershed approach is

*For correspondence. (e-mail: pgsaptarshi@unipune.ernet.in)